Asian Journal of Current Research in Clinical Cancer
ISSN: 3062-4444
2025, Volume 5, Issue 1, Page No: 136-144

Available online at: www.galaxypub.co/page/journals

Galaxy Publication

Galaxy Publication

Next-Generation Sequencing of HPV ctDNA Detects Copy Number Dynamics and Integration as Prognostic Biomarkers in Metastatic Anal Cancer

P. Barth[1*], R. Schroeder[1], C. Müller[1]

[1]Department of Clinical Oncology, Faculty of Medicine, University of Luxembourg, Luxembourg City, Luxembourg.

***E-mail** ✉ luxembourg.clinonc.69@yahoo.com

Received: 12 March 2025; **Revised:** 27 May 2025; **Accepted:** 04 June 2025

ABSTRACT

Traditional circulating HPV DNA tests have had limited scope, so we examined the clinical usefulness of a newly developed next-generation sequencing (NGS)–based HPV ctDNA platform for people with locally advanced or metastatic squamous cell carcinoma of the anal canal (mSCCA). Plasma samples from patients with mSCCA were processed to extract ctDNA, which was analyzed using a 1.4 Mb hybrid-capture panel designed to cover the complete genomic sequences of all 193 known HPV types. A specialized analytic workflow identified HPV genotype, copy number (CN), and integration breakpoints. Seventy-seven plasma specimens collected from 28 individuals with HPV-associated SCCA were reviewed retrospectively. HPV ctDNA was measurable in 26 of these patients (93%), including those with rare viral subtypes. Median HPV CN values were significantly higher in individuals with metastatic disease compared with those with locally recurrent or unresectable tumors ($p = 0.043$). Fluctuations in HPV CN tracked closely with imaging-based treatment response ($p = 0.027$). Viral integration was observed in 23 patients (82%), while the remainder showed patterns consistent with episomal HPV. Patients with more extensive integration (mean ≥1 event across submitted samples) experienced notably poorer overall survival once immunotherapy was initiated (13.6 months compared with 36.0 months; $p = 0.003$). This HPV-focused NGS ctDNA approach demonstrated that changes in HPV CN parallel therapeutic outcomes, and that HPV integration detectable in blood is associated with inferior prognosis.

Keywords: Anal carcinoma, HPV, Circulating tumor DNA

How to Cite This Article: Barth P, Schroeder R, Müller C. Next-Generation Sequencing of HPV ctDNA Detects Copy Number Dynamics and Integration as Prognostic Biomarkers in Metastatic Anal Cancer. Asian J Curr Res Clin Cancer. 2025;5(1):136-44. https://doi.org/10.51847/9rkG7xkfdg

Introduction

Most cases of squamous cell carcinoma arising in the anal canal (SCCA) develop after long-standing infection with human papillomavirus (HPV) [1]. Although vaccines can prevent many HPV-driven cancers, national rates of SCCA in the United States continue to climb [2]. HPV-16 is implicated in the majority of tumors, but other high-risk strains—including HPV-18, HPV-31, HPV-33, HPV-45, and others—also contribute to malignant transformation [3]. Current clinical assays generally rely on p16 immunohistochemistry as an indirect indication of HPV involvement or on in situ hybridization that tests only one or two common HPV types. The rarity of the disease often limits the amount of tumor tissue available for such tests.

While patients with localized SCCA may be cured with combined-modality therapy, those with metastatic or unresectable disease typically have a 5-year overall survival below 40%, with few effective systemic options [4]. There is a considerable unmet need for biomarkers that can guide treatment choices in advanced settings.

The HPV genome encodes six early (E) proteins essential for regulating viral replication and gene expression [5, 6]. Upon infection, the E6 and E7 proteins disrupt p53 and retinoblastoma (Rb), respectively, enabling unchecked cellular replication and, in some cases, tumorigenesis. Integration of HPV DNA into the host genome is common and plays an important role in malignant progression [7]. When integration does not occur, HPV may remain as

cytoplasmic episomes that continue producing viral proteins. Because HPV DNA is present within HPV-driven tumors, detecting HPV ctDNA in blood samples is a feasible strategy for disease monitoring. One common approach—droplet digital PCR (ddPCR)—targets frequent viral regions such as HPV-16 and HPV-18 E7 [8]. ddPCR can identify HPV ctDNA with high sensitivity and follow its changes during treatment [9, 10], but it can measure only a small subset of viral genes and HPV types.

To broaden the clinical utility of liquid biopsy in HPV-associated cancers, we developed an NGS-based ctDNA assay capable of capturing the full HPV genome, identifying the involved subtype(s) without prior assumptions, and detecting viral integration sites. Broad NGS-based HPV ctDNA assays have been tested in cervical and oropharyngeal cancers, showing higher sensitivity compared with ddPCR [11]. Their role, however, has not been defined in advanced anal cancer. The present report describes how a hybrid-capture HPV ctDNA NGS platform performed in a prospective cohort of patients with incurable SCCA undergoing systemic therapy.

Materials and Methods

Patients

As part of IRB-approved prospective protocols at the University of Texas MD Anderson Cancer Center (MDA) and the National Cancer Institute (NCI), peripheral blood was drawn from individuals presenting with either newly identified or previously treated metastatic squamous cell carcinoma of the anal canal, as well as from those whose tumors were not amenable to surgical removal. Between September 2015 and June 2019, each participant provided 1–4 blood specimens obtained during the course of systemic therapy.

Two sets of banked plasma were available. The first consisted of 20 patients treated at MDA with diverse therapeutic regimens; the second included 8 participants from a phase II nivolumab monotherapy study (NCI9673, part A; NCT02314169) designed for treatment-refractory metastatic or unresectable SCCA.

Therapeutic exposure in the MDA series covered: nivolumab (n = 5), ipilimumab combined with nivolumab (n = 4), pembrolizumab (n = 2), atezolizumab with bevacizumab (n = 2, NCT03074513), and a regimen of durvalumab plus the HPV-16/18 E6/E7 DNA vaccine MEDI-0457 (n = 1, NCT03439085). Clinical information—including prior therapy, imaging-based assessment, and follow-up—was extracted from electronic records. Tumor response was determined by the managing oncologist and reviewed in multidisciplinary settings; the RECIST v1.1 criteria were specifically applied within the NCI cohort. Comprehensive baseline and treatment data were available only for the MDA patients, while the NCI group had limited but essential variables (age, metastatic distribution, progression dates on study therapy, and follow-up) recorded. Written informed consent was obtained from all participants prior to any optional research use of biospecimens.

Sample handling and bioinformatic analysis

Plasma samples previously stored at −80°C were thawed using a room-temperature water bath, followed by centrifugation at 1600× g for 10 minutes to eliminate residual particulate matter. Circulating tumor DNA was purified from the cleared plasma using the QIAsymphony DSP Circulating DNA Kit operated on the QIAsymphony platform (Qiagen, Germantown, MD, USA).

For library construction, 5–30 ng of input material underwent end-repair and adaptor ligation using the NEBNext Ultra II DNA Library Prep Kit (New England Biolabs, Ipswich, MA, USA). Dual-index molecular barcodes synthesized by IDT (Coralville, IA, USA) were incorporated, and adaptor-ligated fragments were isolated with SPRIselect beads. After amplification, the libraries were enriched via hybrid capture with a custom HPV panel.

This in-house panel comprised 34,048 probes that collectively target 1.432 Mb of viral genome, representing 193 distinct HPV types, and also included TP53 as a human internal control. Post-capture washing was followed by a second amplification, bead purification, and elution in low-TE buffer. Library concentrations were determined using the Agilent 4200 TapeStation, pooled, and sequenced on the Illumina NextSeq550 following manufacturer protocols.

A custom computational workflow processed the sequencing output. FASTQ reads were collapsed using dual unique molecular identifiers to generate consensus error-corrected sequences. These were aligned to both human and HPV reference genomes using BWA and Bowtie2. Internal software modules then determined HPV genotype, viral genome coverage, and estimated viral copy number via read-depth calculations. Structural variant detection with GRIDSS was used to identify HPV–host integration breakpoints.

Statistical analysis

Descriptive summaries were generated for all clinical and demographic variables, presenting categorical data as counts and percentages and continuous data using median values. The Mann–Whitney U test was applied to compare continuous measurements, whereas Fisher's exact test was used for categorical comparisons.

Survival distributions were evaluated using the Kaplan–Meier approach. Progression-free survival (PFS) was defined as the interval from therapy initiation until radiologic progression or death, and overall survival (OS) as the duration from diagnosis or treatment onset to death from any cause. Cox proportional hazards models were employed to examine relationships between clinical variables and time-to-event outcomes. As the study was exploratory and descriptive, no adjustments were made for multiple hypothesis testing, and statistical significance was set at $p \leq 0.05$. All analyses were carried out using SPSS version 29.

Results and Discussion

Patient characteristics

Blood samples for assessing HPV copy number and integration in ctDNA were prospectively collected from 28 individuals, producing 77 total analyzable specimens (each person contributed between 1 and 4 samples). **Table 1** summarizes their baseline demographics. The median age was 60 years. Most had previously undergone therapy for locoregional disease before later developing advanced or nonresectable recurrence. Twenty-two patients (71%) received anti–PD-1 treatment; the majority were managed with single-agent nivolumab (n = 13), while four received a nivolumab–ipilimumab combination for metastatic disease.

Table 1. Baseline characteristics.

Characteristic	MDA Group (%), n = 20	NCI Group (%), n = 8
Median age (range, y)	60 (44–72)	61 (36–70)
Gender		
Male	4 (20%)	
Female	16 (80%)	
Initial staging at diagnosis		
Locoregional	14 (70%)	
Metastatic	6 (30%)	
HPV status		
p16+ according to immunohistochemistry	20 (100%)	
Treatments for advanced disease		
5-fluorouracil and cisplatin	9 (45%)	
Carboplatin and Paclitaxel	9 (45%)	
Immunotherapy	12 (60%)	
Cetuximab	4 (20%)	
Site of recurrence or metastases		
Locoregional only	7 (35%)	3 (38%)
Distant	13 (65%)	5 (63%)
Median follow-up from metastatic disease (months)	26.9	-

HPV copy number changes with treatment

Among the 26 patients with measurable circulating HPV, the highest copy number recorded for each individual was greater in those who had distant metastases compared with those who presented only with locally advanced or unresectable tumors. The median ctDNA HPV quantity for the locoregional subgroup (n = 9) was 1805 copies [SD: 15,530], whereas the metastatic cohort (n = 17) showed a median of 9462 copies [SD: 15,243] ($p = 0.043$) **(Figure 1a)**.

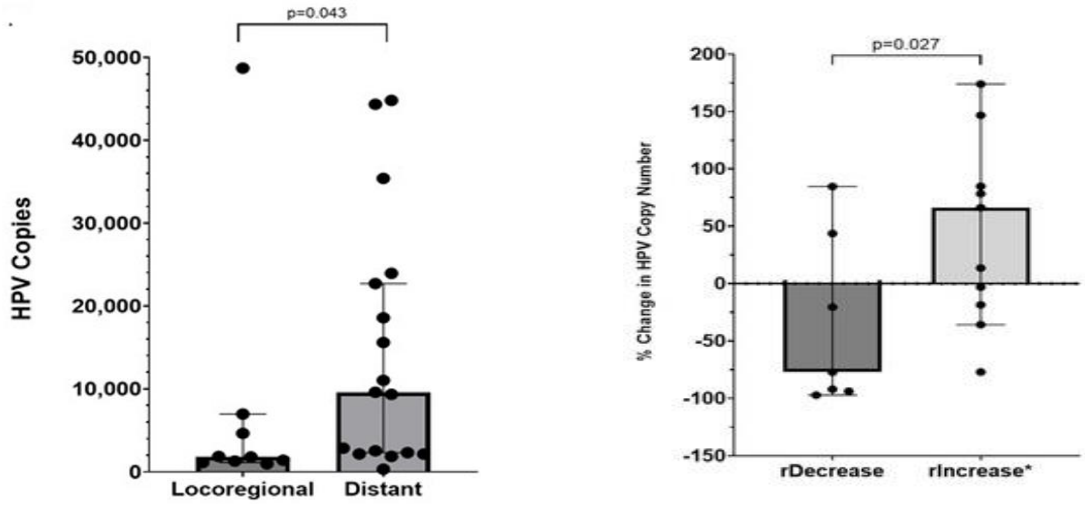

a) b)

Figure 1. HPV copy number and treatment-related findings

Panel a presents the *peak* HPV copy count measured for each individual, grouped into locoregional cases and those with distant metastases. The vertical bar marks the group median, and each marker corresponds to one patient.

Panel b shows the *percent shift* in HPV copies for matched blood samples, categorized by whether imaging indicated disease regression (rDecrease) or worsening (rIncrease). A single outlier with a 1692% rise is omitted.

Fifteen participants contributed multiple blood draws, enabling treatment-course monitoring alongside available imaging interpretations. Altogether, 18 matched intervals met the requirement of being ≥28 days apart, allowing assessment of how ctDNA HPV levels varied with therapy. The midpoint between draws was 82 days, with a span ranging from 28 to 274 days.

A clear pattern emerged when ctDNA changes were compared with radiographic evaluations in patients with noncurable SCCA. Imaging suggested tumor reduction in 7 paired intervals and disease enlargement in 11. As illustrated in **Figure 1b**, the group showing radiographic improvement demonstrated a median drop of 77.3% in HPV copies, whereas those whose scans indicated progression exhibited a median rise of 66.2% ($p = 0.027$).

HPV variants and detection of integration events

HPV genotyping and mapping of integration sites were available for the full group (MDA and NCI datasets). In addition to HPV-16, several other high-risk genotypes were identified in plasma: HPV-18 (n = 2), HPV-45 (n = 2), HPV-73 (n = 1), and HPV-91 (n = 1), collectively seen in five patients **(Table 2)**. Four individuals exhibited HPV-16 concurrently with one of these additional types, and one patient carried both HPV-18 and HPV-45.

Across 70 plasma samples, 298 integration breakpoints were documented. The median number of integrations per sample was two (range: 0–46). Twenty-six samples contained HPV without evidence of integration, consistent with episomal viral DNA.

Table 2. HPV types detected from ctDNA.

HPV Type	# of Patients (n = 28)
HPV-16	25
HPV-18	2
HPV-45	2
HPV-73	1
HPV-91	1

We detected 127 HPV-associated integration sites distributed among 27 genes in the genomic regions examined **(Table 3)**.

A set of eight recurrent integration zones—defined by having ≥2 breakpoints within 500 kb—was observed near the following loci **(Figure 2a)**: ADAM7, SKAP2, TBL1XR1, CHRM3, GALK1, ITGB4, THRDE, GRK5, EIF3A, and NFIB.

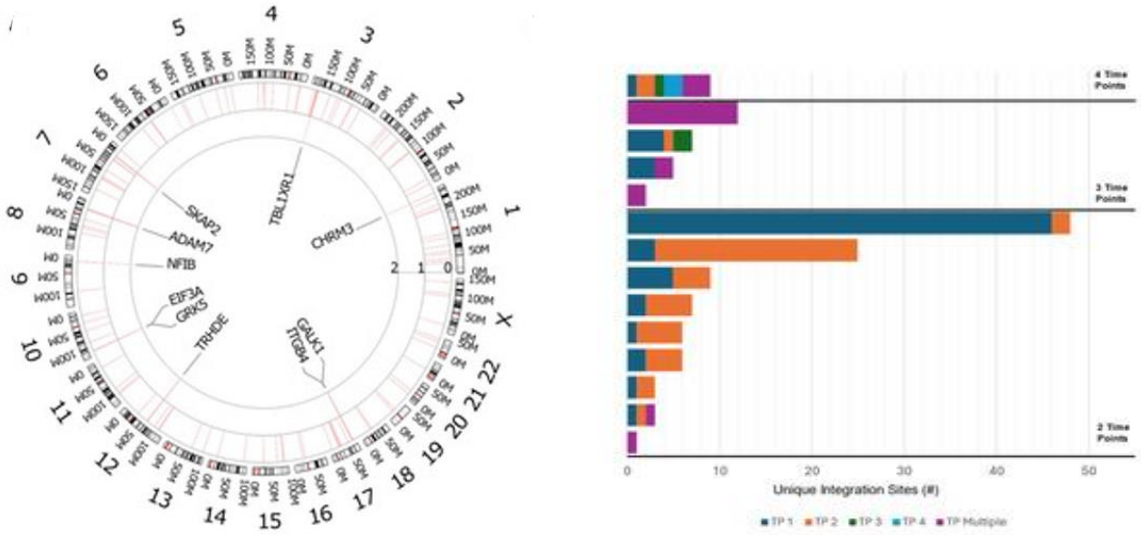

a) b)

Figure 2. Integration clusters and temporal agreement. (a) Shows how HPV integration points are spread across the genomes of all participants with measurable viral DNA (n = 26). Chromosomes form the outer ring, labeled in megabase units, while the inner ring uses red bars to indicate how often integration occurred; histogram values correspond to sample counts. Genes situated within <500 kb of regions with a high integration burden are annotated.

(b) Depicts the total number of distinct integration sites identified in patients who contributed ≥2 blood draws. Each bar corresponds to one individual, and the x-axis shows the count of separate integration locations. Colors indicate whether a locus appeared at a single time point (TP) or persisted across multiple TPs.

Table 3. Protein-coding genes encompassing HPV integration breakpoints.

Gene Symbol	Chromosome	Rephrased Description
CHRM3	1	muscarinic acetylcholine receptor subtype 3
FMN2	1	formin family protein 2
GREM2	1	member of the DAN/BMP-antagonist family, known as gremlin 2
TBL1XR1	3	X-linked transducin-like protein 1 receptor
SKAP2	7	src-associated adaptor/phosphoprotein 2
ADAM7	8	metalloprotease-related ADAM family protein 7
ADAMDEC1	8	ADAM-decysin family member 1
NFIB	9	nuclear factor I, subtype B
EIF3A	10	largest subunit (A) of the eukaryotic translation initiation factor 3 complex
FAM45A	10	protein from sequence-similarity family 45, type A
GRK5	10	G-protein receptor kinase 5
NANOS1	10	nanos 1, ortholog of the Drosophila gene
PRDX3	10	mitochondrial peroxiredoxin isoform 3
SFXN4	10	sideroflexin family member 4
CASKIN2	17	CASK-binding scaffold protein 2
GALK1	17	galactokinase enzyme 1
ITGB4	17	beta-4 integrin subunit
KIAA0195	17	protein encoded by the KIAA0195 locus
LLGL2	17	homolog of Drosophila lethal-giant-larvae gene, type 2
MYO15B	17	unconventional myosin XVB

RECQL5	17	RecQ helicase family member 5
SAP30BP	17	protein that associates with SAP30
SMIM5	17	small membrane-embedded protein 5
SMIM6	17	small membrane-embedded protein 6
TSEN54	17	subunit 54 of the tRNA-splicing endonuclease complex

Most individuals with serial sampling exhibited different integration profiles at each time point. Among the 14 patients who had integration calls in more than one sample, 6 had at least one site that recurred across multiple draws.

HPV integration as a prognostic marker

To determine whether HPV integration could serve as a prognostic classifier after systemic therapy for incurable SCCA, all patients with detectable ctDNA HPV were assigned to either an "HPV integration" or "HPV non-integration" category. Patients were considered non-integration cases if no integration was observed in any sample or if their average count across multiple samples was less than 1 (n = 9). All remaining individuals were categorized as integration-positive (n = 19).

Survival outcomes were then examined across all administered systemic treatments (chemotherapy, immunotherapies, and targeted agents such as cetuximab). In the MDA cohort (n = 20), the median PFS on first-line metastatic chemotherapy was 8.0 months (95% CI: 0–16) for the integration group compared with 11 months (95% CI: 4.2–17.7) for the non-integration group (HR: 0.59; 95% CI: 0.20–1.72; p = 0.33) **(Figure 3a)**. Median OS from metastatic diagnosis was 24.3 months (95% CI: 5.3–43.3) for integration-positive patients, while the non-integration cohort had not yet reached median OS (HR: 0.30; 95% CI: 0.10–0.92; p = 0.09) **(Figure 3b)**.

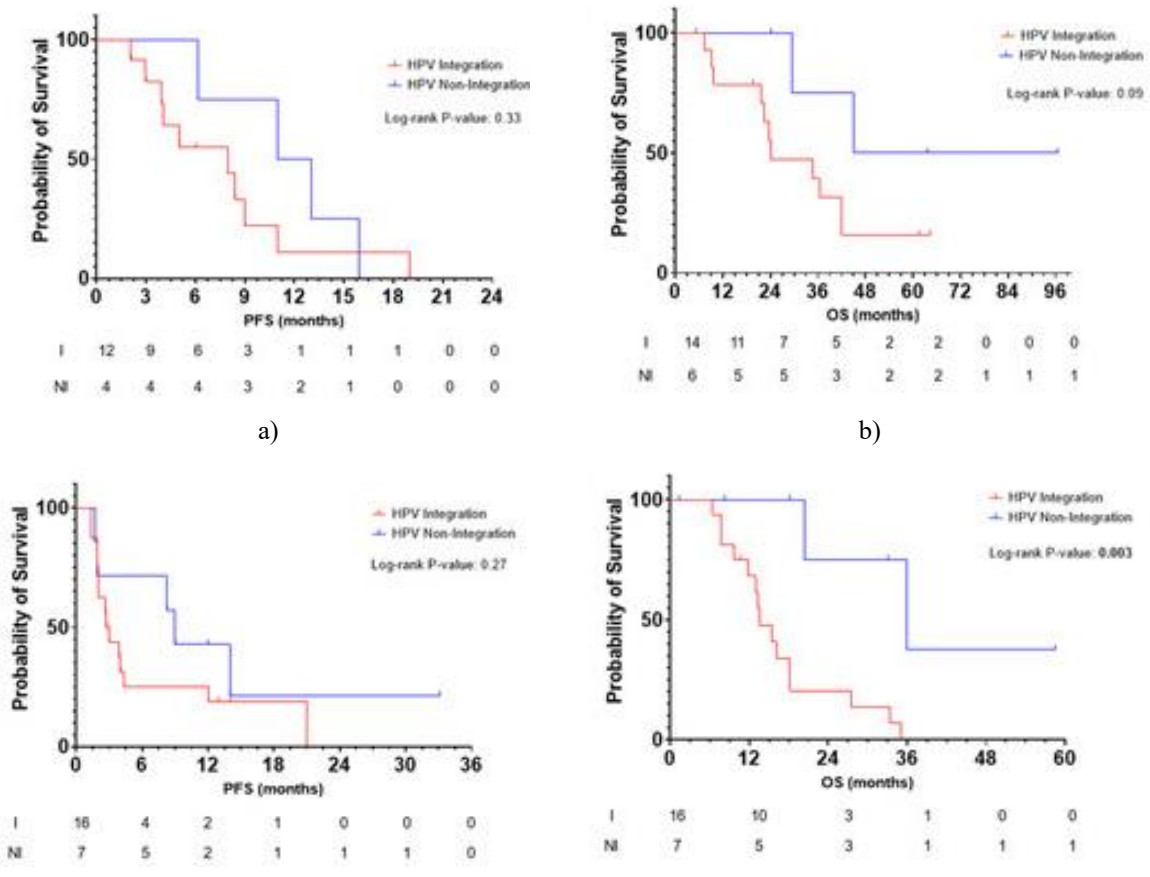

Figure 3. Survival by HPV Integration Category

Figure 3 presents outcomes stratified by HPV integration: panels A and B illustrate PFS and OS under all systemic treatments, while panels C and D show PFS and OS beginning at the initiation of immune checkpoint blockade. I = integration; NI = non-integration.

We then assessed survival patterns in relation to HPV integrationm specifically among the patients treated with immunotherapy for whom adequate information was available (MDA + NCI cohorts; n = 23). In this subset, the median PFS from the start of PD(L)-1 inhibitor therapy for metastatic disease was 2.8 months (95% CI: 2.1–3.5) for the integration group compared with 9.0 months (95% CI: 7.2–10.9) for the non-integration group (HR: 0.58; 95% CI: 0.23–1.45; p = 0.27) **(Figure 3c)**. Median OS measured from the initiation of PD(L)-1 therapy was 36.0 months (95% CI: 10.5–16.8) in integration-positive cases versus 13.6 months (95% CI: 12.8–59.1) for the non-integration group (HR: 0.21; 95% CI: 0.06–0.42; p = 0.003) **(Figure 3d)**, favoring the non-integration cohort. When adjusted in a multivariable model that included age and initial extent of disease (locoregional vs. metastatic), the relationship between integration status and OS after starting immunotherapy remained significant (HR: 0.17; 95% CI: 0.03–0.90; p = 0.037).

Minimally invasive testing, such as ctDNA analysis, offers an important alternative for patients with uncommon cancers like SCCA, where tumor tissue is often difficult to collect. In this investigation, we demonstrate that measuring circulating HPV DNA using a sequencing strategy tailored to HPV not only mirrors disease burden but also aligns with treatment response in advanced or incurable SCCA. This expands the clinical scope of liquid biopsy for anal cancer beyond HPV-targeted ddPCR by enabling broad genomic interrogation without depending on tumor tissue. Notably, HPV integration could be detected through ctDNA analysis, and this feature appeared to carry prognostic relevance after the introduction of immunotherapy. These findings reinforce similar observations in other HPV-associated malignancies, in which whole-genome HPV ctDNA profiling has shown feasibility for disease monitoring [12].

Earlier clinical work in advanced anal cancer primarily applied ddPCR-based assays that capture short HPV sequences (100–200 bp), limited to common HPV subtypes [13]. Wide-range NGS assays theoretically offer higher sensitivity because they can detect less common HPV strains. Although our pilot cohort was small, every patient in this study had detectable HPV ctDNA. Supporting this concept, comparative analyses in cervical and oropharyngeal cancers have shown strong quantitative agreement between ddPCR and NGS for HPV copy number measurement, with NGS outperforming ddPCR at lower viral loads [11, 14]. One previously reported NGS panel used in localized anal cancer included two primer sets spanning portions of eight high-risk HPV genomes [15]. In contrast, our panel was designed to capture all HPV genotypes, enabling the detection of multiple high- and low-risk types at various time points. Importantly, it also identified integration events that may hold biological or prognostic value.

Because no validated blood-based markers currently exist to approximate tumor volume or therapeutic effect beyond imaging, circulating HPV DNA may fill a meaningful gap in care for advanced anal cancer. Supporting this idea, the Epitopes-HPV02 study—evaluating DCF chemotherapy—showed associations between HPV ctDNA levels and both disease extent and dynamic response using ddPCR [10]. Most commonly, HPV ctDNA has been evaluated for its role in predicting recurrence after chemoradiotherapy for localized disease [9, 15, 16]. In one series, all three patients with detectable pre- and post-treatment HPV ctDNA subsequently relapsed within six months [9]. For metastatic disease, ctDNA HPV measurements could serve several functions: early response tracking ahead of routine imaging, detection of minimal residual disease, or clarifying ambiguous radiographic findings in patients with durable immunotherapy responses.

In the present study, HPV DNA integration appeared to show an association with long-term outcomes after systemic therapies, particularly immunotherapy. The Epitopes-HPV02 trial similarly reported a trend toward inferior PFS on DCF among integration-positive cases (median 10.6 vs. 19.5 months), although not statistically significant [17]. Mechanistically, several analyses suggest that HPV integration modulates immune biology. In a TCGA cohort of HPV-positive head and neck cancers, patients lacking detectable integration (identified via RNA fusion transcripts) experienced better OS compared with integration-positive cases [18]. These integration-negative tumors showed stronger immune-cell signatures, including enhanced CD3+, CD4+, CD8+, NK-cell, T-reg, B-cell, and CD34+ signals. Additional studies in HPV-positive HNSCC have identified recurrent hotspots near MYC and PDL1, with integration linked to amplified gene expression [19, 20]. In cervical adenocarcinomas, insertions at STARD3 or ERBB2 correlated with elevated protein levels of those genes [21]. Although the hotspots observed in our analysis differed from those previously reported in HNSCC or cervical cancer—likely reflecting sample size or biology—several genes mapped in this study have documented relevance to metastasis and tumor

aggressiveness [23-30]. Collectively, these findings suggest that viral integration modifies host oncogene regulation and may influence therapy resistance, though the specific consequences of integration at different genomic loci remain uncertain.

This study has limitations. The sample size was modest, and detailed clinical histories were incomplete for several participants, preventing consistent assessment of survival from diagnosis or stratification by multiple treatment lines. As a result, whether the OS advantage observed in the non-integration group reflects true biological prognosis or differences in subsequent therapies is unclear, particularly since no established post-immunotherapy therapies exist. Blood sampling intervals varied widely, limiting the ability to define a standardized quantitative biomarker. There were also instances in which HPV ctDNA did not match radiographic findings, emphasizing the inherent variability of ctDNA influenced by pre-analytical and biological factors.

Conclusion

In summary, this study demonstrates that whole-genome HPV ctDNA sequencing is clinically informative for patients with advanced anal cancer, correlates with treatment activity, and identifies HPV integration patterns that may hold prognostic significance. These observations support further prospective evaluation of this assay, including validation of HPV integration detected in ctDNA as a potential prognostic biomarker.

Acknowledgments: None

Conflict of Interest: None

Financial Support: None

Ethics Statement: None

References

1. Lin C, Franceschi S, Clifford GM. Human papillomavirus types from infection to cancer in the anus, according to sex and HIV status: A systematic review and meta-analysis. Lancet Infect Dis. 2018;18(2):198–206.
2. Deshmukh AA, Suk R, Shiels MS, Sonawane K, Nyitray AG, Liu Y, et al. Recent trends in squamous cell carcinoma of the anus incidence and mortality in the United States, 2001–2015. J Natl Cancer Inst. 2020;112(8):829–38.
3. Palefsky JM, Holly EA, Ralston ML, Jay N. Prevalence and risk factors for human papillomavirus infection of the anal canal in human immunodeficiency virus (HIV)-positive and HIV-negative homosexual men. J Infect Dis. 1998;177(2):361–7.
4. Eng C, Ciombor KK, Cho M, Dorth JA, Rajdev LN, Horowitz DP, et al. Anal cancer: Emerging standards in a rare disease. J Clin Oncol. 2022;40(25):2774–88.
5. Schiffman M, Doorbar J, Wentzensen N, de Sanjosé S, Fakhry C, Monk BJ, et al. Carcinogenic human papillomavirus infection. Nat Rev Dis Primers. 2016;2(1):16086.
6. Akagi K, Symer DE, Mahmoud M, Jiang B, Goodwin S, Wangsa D, et al. Intratumoral heterogeneity and clonal evolution induced by HPV integration. Cancer Discov. 2023;13(4):910–27.
7. McBride AA, Warburton A. The role of integration in oncogenic progression of HPV-associated cancers. PLoS Pathog. 2017;13(4):e1006211.
8. Lin G, Li J. Circulating HPV DNA in HPV-associated cancers. Clin Chim Acta. 2023;542:117269.
9. Cabel L, Jeannot E, Bieche I, Vacher S, Callens C, Bazire L, et al. Prognostic impact of residual HPV ctDNA detection after chemoradiotherapy for anal squamous cell carcinoma. Clin Cancer Res. 2018;24(23):5767–71.
10. Bernard-Tessier A, Jeannot E, Guenat D, Debernardi A, Michel M, Proudhon C, et al. Clinical validity of HPV circulating tumor DNA in advanced anal carcinoma: An ancillary study to the Epitopes-HPV02 trial. Clin Cancer Res. 2019;25(6):2109–15.

11. Leung E, Han K, Zou J, Zhao Z, Zheng Y, Wang TT, et al. HPV sequencing facilitates ultrasensitive detection of HPV circulating tumor DNA. Clin Cancer Res. 2021;27(21):5857–68.
12. Elasifer H, Amukwaya MMN, Bhatia R, Cuschieri K, Gregory JM. The role of circulating viral and tumour DNA in the diagnosis and management of HPV associated anogenital cancers, a systematic review and meta-analysis. J Clin Virol. 2023;164:105469.
13. Chatfield-Reed K, Roche VP, Pan Q. cfDNA detection for HPV+ squamous cell carcinomas. Oral Oncol. 2021;115:104958.
14. Naegele S, Ruiz-Torres DA, Zhao Y, Goss D, Faden DL. Comparing the diagnostic performance of quantitative PCR, digital droplet PCR, and next-generation sequencing liquid biopsies for human papillomavirus-associated cancers. J Mol Diagn. 2024;26(3):179–90.
15. Lee JY, Cutts RJ, White I, Augustin Y, Garcia-Murillas I, Fenwick K, et al. Next generation sequencing assay for detection of circulating HPV DNA (cHPV-DNA) in patients undergoing radical (chemo)radiotherapy in anal squamous cell carcinoma (ASCC). Front Oncol. 2020;10:505.
16. Damerla RR, Lee NY, You D, Soni R, Shah R, Reyngold M, et al. Detection of early human papillomavirus–associated cancers by liquid biopsy. JCO Precis Oncol. 2019;3:1–17.
17. Debernardi A, Meurisse A, Prétet JL, Guenat D, Monnien F, Spehner L, et al. Prognostic role of HPV integration status and molecular profile in advanced anal carcinoma: An ancillary study to the Epitopes-HPV02 trial. Front Oncol. 2022;12:941676.
18. Koneva LA, Zhang Y, Virani S, Hall PB, McHugh JB, Chepeha DB, et al. HPV integration in HNSCC correlates with survival outcomes, immune response signatures, and candidate drivers. Mol Cancer Res. 2018;16(1):90–102.
19. Mainguené J, Vacher S, Kamal M, Hamza A, Masliah-Planchon J, Baulande S, et al. Human papilloma virus integration sites and genomic signatures in head and neck squamous cell carcinoma. Mol Oncol. 2022;16(14):3001–16.
20. Symer DE, Akagi K, Geiger HM, Song Y, Li G, Emde AK, et al. Diverse tumorigenic consequences of human papillomavirus integration in primary oropharyngeal cancers. Genome Res. 2022;32(1):55–70.
21. Bi Y, Hu J, Zeng L, Chen G, Cai H, Cao H, et al. Characteristics of HPV integration in cervical adenocarcinoma and squamous carcinoma. J Cancer Res Clin Oncol. 2023;149(6):17973–86.
22. Kamal M, Lameiras S, Deloger M, Morel A, Vacher S, Lecerf C, et al. Human papilloma virus (HPV) integration signature in cervical cancer: Identification of MACROD2 gene as HPV hot spot integration site. Br J Cancer. 2021;124(4):777–85.
23. Denny SK, Yang D, Chuang CH, Brady JJ, Lim JS, Grüner BM, et al. Nfib promotes metastasis through a widespread increase in chromatin accessibility. Cell. 2016;166(4):328–42.
24. Wang Y, Li J, Wen S, Yang X, Zhang Y, Wang Z, et al. CHRM3 is a novel prognostic factor of poor prognosis in patients with endometrial carcinoma. Am J Transl Res. 2015;7(5):902–11.
25. Wang S, Liu Y, Yao M, Jin J. Eukaryotic translation initiation factor 3a (eIF3a) promotes cell proliferation and motility in pancreatic cancer. J Korean Med Sci. 2016;31(10):1586–94.
26. Kuranami S, Yokobori T, Mogi A, Altan B, Yajima T, Onozato R, et al. Src kinase-associated phosphoprotein2 expression is associated with poor prognosis in non-small cell lung cancer. Anticancer Res. 2015;35(4):2411–5.
27. Takagane K, Umakoshi M, Itoh G, Kuriyama S, Goto A, Tanaka M. SKAP2 suppresses inflammation-mediated tumorigenesis by regulating SHP-1 and SHP-2. Oncogene. 2022;41(9):1087–99.
28. Gambardella J, Franco A, Giudice CD, Fiordelisi A, Cipolletta E, Ciccarelli M, et al. Dual role of GRK5 in cancer development and progression. Transl Med UniSa. 2016;14:28–37.
29. Du R, Li K, Guo K, Chen Z, Zhao X, Han L, et al. Two decades of a protooncogene TBL1XR1: From a transcription modulator to cancer therapeutic target. Front Oncol. 2024;14:1309687.
30. Huang W, Fan L, Tang Y, Chi Y, Li J. A pan-cancer analysis of the oncogenic role of integrin beta4 (ITGB4) in human tumors. Int J Gen Med. 2021;14:9629–45.